Beam Diagnostic for the Rare Isotope Accelerator Facility

Dan Shapira
Physics Division, Oak Ridge National Laboratory,† Oak Ridge, Tennessee

Development of beam diagnostic devices at the HRIBF for radioactive beams is an ongoing effort (Ref. 1) that will also benefit operations at future Rare Isotope Accelerator facility. I shall provide a brief description of devices we have developed, list the needs they addressed and what additional development and enhancement we perceive might become useful at the Rare Isotope Accelerator facility.

Diagnostics for High Beam Intensities

We have been using a modified version of a residual gas beam profile monitor (RGBPM). In this detector gas molecules in the evacuated beam pipe are ionized by the passing beam particles and the ions are extracted by electric field transverse to the beam direction. The position of these extracted ions are then recorded in two-dimensional position sensitive detectors (see Ref. 2 and Fig. 1a). This device samples the projection of the beam profile in one plane. It is customary to use two such devices to provide two orthogonal projections of the beam path. What makes this device attractive, in general, is its low mass (thin). The fact that the beam is not deposited in the detector is a plus for radioactive ion beams.

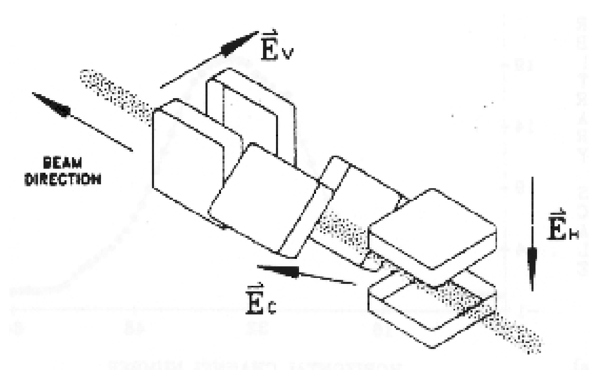

Fig. 1a. Arrangement of detectors employed with two dimensional profiling device.

Initially, we developed this device to provide continuous monitoring of the radioactive beam trajectory in front of experimental stations. The expected beam intensities were low so in our application emphasis was placed on extracting full 3-D information on the position of the ionizing event in a single sample and on enhancing the sampling rate. In our version of the RGBPM, the extracted ion's position signal is supplemented by drift time to provide full 3D position information of the ionization site and allows direct viewing of the beam profile (See Fig. 1b and Ref. 3). We operate this device with a small

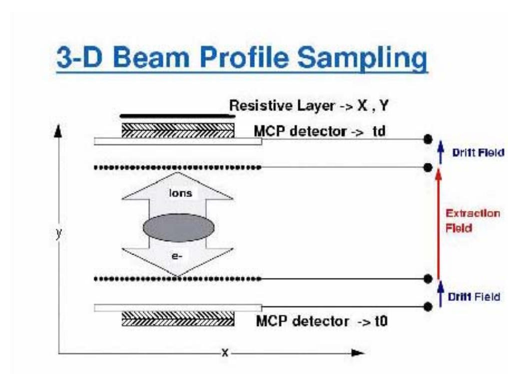

Fig. 1b. Schematic diagram showing the operation of the RGBPM with recording ionization site in 3-D. Beam (z pointing out of plane.

† Managed by UT-Battelle, LLC, for the U.S. Department of Energy under contract DE-AC05-00OR22725.

addition of trace gas that serves to increase the sampling rate and also helps relate ion drift time to position. For example, we maintained a steady leak of N^2 gas that raised the ambient pressure to $5*10^{-6}$ Torr and were able to obtain good samples of the beam profile at rates near $5*10^4$ particles/sec (see Fig. 2). The position resolution is ~1-2mm in the ion drift direction and far better in the plane perpendicular to the drift direction. A different type of beam detector that can also be fairly thin, is capable of superior position and timing resolution, and is more appropriate for low beam intensities supplanted this beam profile detector and will be described later.

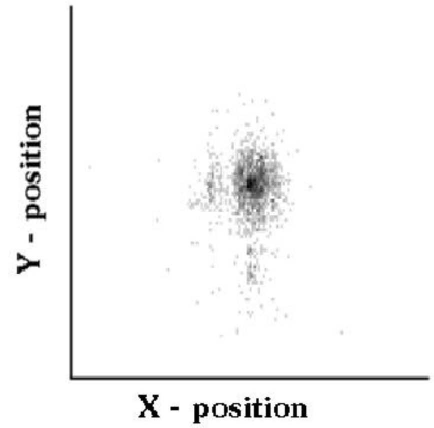

Fig. 2. Two-dimensional beam profile obtained with a beam of 10^5 ^{69}As ions per second.

The sampling probability in the RGBPM is governed by the probability of an ionizing collision occurring between the beam and the gas molecules in the detector sensitive volume traversed by the beam. This probability can be easily controlled by changing ambient pressure as demonstrated in the data of Fig. 3. Other parameters controlling this probability include the physical size of the detector and the cross section for ionization of the ambient gas molecules (mostly He and H_2) by the passing beam.

We propose to use an RGBPM to provide continuous monitoring of the intensity and profile of the high-intensity driver beam on its way to the target. The design should be modified to accommodate the high beam rates. We may forgo the drift time measurements and have two identical devices that extract the ions from the collision to provide two orthogonal projections of the beam trajectory. The sampling region should be a narrow strip (~1mm × 50mm) requiring only a one-dimensional position measurement of the ion hit position along the direction of the 50-mm slot (See Fig. 4). A micro-channel plate detector records the position where the ion hit along an anode plated with one or few position sensing wires (either by charge division or signal delay).

An order of magnitude estimate of the ionization probability can be obtained by calculating the energy loss of the beam traversing the sampling region and dividing it by the mean ionization potential. The energy loss can be calculated with the Bethe-Bloch formula for specific energy loss,

$$-dE/dx = 0.3071*\left(z^2 Z/A\beta^2\right)*\ln\left[2m_e c_2 \gamma^2 \beta^2/I + \right.$$
relativistic and screening corrections],

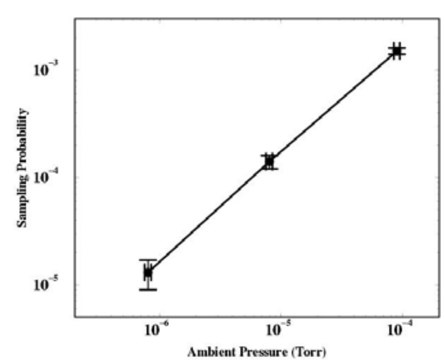

Fig. 3. Sampling rate as a function of ambient pressure.

where $\beta = v/c, \gamma = \sqrt{1-\beta^2}$, z=projectile charge, Z=target charge, m_e=electron mass, I=ionization potential of the residual gas atom and c=velocity of light in vacuum.

For 60-MeV protons passing through 1 mm of residual H_2 gas at a pressure of 10^{-7} Torr at normal STP, we expect an ionization probability of $\sim 2*10^{-9}$ per beam particle or $\sim 10^4$ samples per second per 1µA of proton beam. Better estimates can be gotten from an understanding of the atomic processes that cause ionization.

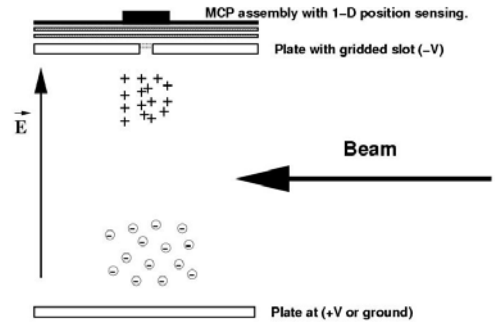

Fig. 4. Proposed RGBPM for high-intensity beams has a short sampling region.

The proposed device looks simple and one may be tempted to just build it when the need arises. There are however several issues that should be addressed and may take some time and effort. Some that come to mind are listed below:

1) Radiation hardness – how far from the actual ISOL target do we have to station this device so that it can be operated for an extended length of time?
2) Make sure there are no surprises at high beam intensities. After full acceleration to 10 KV, a H^+ ion can cover 0.13 cm in one nanosecond. Space charge screening may become a problem. Some questions can be answered at the library, others may need further study.
3) Sampling probability at high rates. The lifetime for the n = 3 state in Hydrogen is few nanoseconds and 100 µA beam particles arrive at ~1 femto second intervals. Can this affect the probability of two stage processes? Do we know enough about the dependence of atomic cross section on beam energy?
4) Study the best way to measure position signals. This would depend on the rate we want to handle and the resolution needed.

Some of these tests can be performed at the HRIBF where we have a driver that can deliver 10 µA beams.

Diagnostics for Low Beam Intensities

At present day RIB facilities delivered beam intensities rarely exceed few Mhz rates therefore our efforts at HRIBF concentrated on detectors that could provide beam count and profile measurements starting at a few counts/sec leading up to a few million counts/sec. The emphasis was on providing a detector with good position and timing resolution that will have low mass (i.e., can stay in the beam) and operate well at rates up to few Mhz. The detectors we used are all based on the idea of detecting secondary emissions (electrons) from the interaction of the passing beam particles. A typical detector is shown in Fig. 5 (Ref. 4). These detectors can operate with very thin foils but in general they have fairly poor position resolution (no better then 5% of the electron drift distance) and suffer from non-Gaussian peak shapes with very long tails. Our studies have shown that the main culprit is the transverse components of the velocity distribution of the secondary electrons (Ref. 5). It turns out that a combination of magnetic and electric fields, running approximately parallel to each other can provide more precise guiding of the electrons from the site of beam incidence on the foil to the detector (See Fig. 6). The modified detector is shown in Fig. 7 (Ref. 6). The two permanent magnets determine the field strength at the foil, the detector plane and in between. As long as the magnetic field is strong enough to maintain adiabatic conditions electrons will spiral and move along the magnetic field lines in a pattern shown in Fig. 6. The end result is that the magnetic field strength near the foil determines position resolution and the ratio of magnetic field strengths at the foil and the detector will determine the electron trajectory and the image magnification.

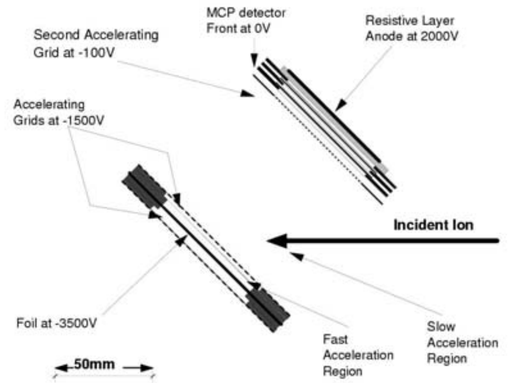

Fig. 5. The modified position sensitive timing detector (PSTD).

Fig. 8 shows how well the idea works. Both patterns were obtained with the same mask and one can see remarkable improvements in picture quality. Note the smaller 1/4 and 1/2 mm holes are not visible in the top part mainly due to the large tail in the position spectrum. Another significant improvement in this detector is that we do not rely on strong and immediate acceleration of the electrons to achieve high resolution and therefore do not need any of the grids near the foil.

What we would like to concentrate on in the future are several improvements.

1) Stronger magnetic fields. Aside from improving position resolution this will allow us to increase the electrostatic voltage for accelerating the electrons without violating adiabaticity.

2) Improve performance at high counting rate. Only recently were we able to maintain position resolution at rates up to 1.5 Mhz. Can we go further? Is there a need for it?

3) Build detectors with larger aperture. We can try by combining several detectors or/and de-magnify the projected image.

So far these detectors have not been installed at the position of the waist in the beam path, but many experimental stations have installed this detector. In many cases, depending on beam species and energies, the detectors have near 100% efficiency. In such cases, they can be used for beam tracking and can be made part of the trigger in experiments. There are several instances that the superb position and timing resolution of these detectors elevated them to integral parts of the experiment. The efficiency of this detector is determined by

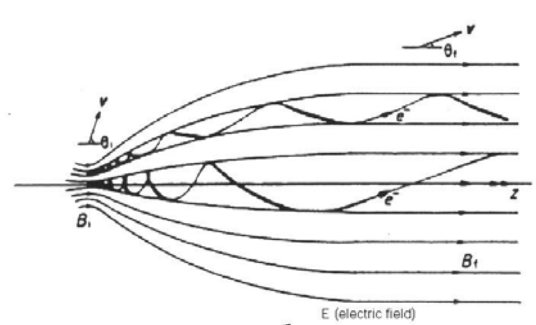

Fig. 6. Diagram shows the helical motion of an electron moving in a magnetic field that changes gradually from a strong field B_i to a weak field B_f.

the probability of electrons being emitted upon ion impact. In this device, we collect mostly electrons emitted near the surface and the number of these correlates with the specific energy loss. This provides a clear link between efficiency and beam energy and species. A few examples that we tested are shown in Table 1. Good working conditions are when there are more then 10 electrons emitted per collision. In such cases, the signal is well above noise (1 or 2 electron level) and are always above a comfortable threshold regardless of gain changes on the MCP (due to rate).

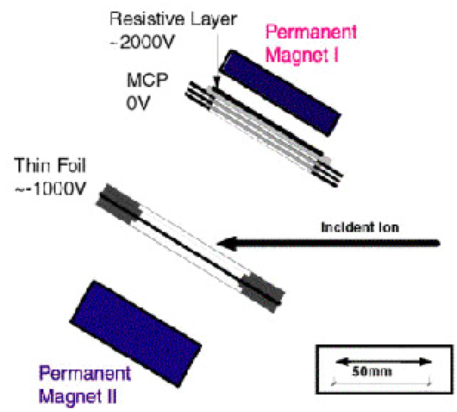

Fig. 7. The detector from Fig. 4 is shown here with the addition of two permanent magnets. The strength of the magnetic field near the foil determines the overall position resolution that can be achieved. The ratio of the magnetic field strength in front of the detector to that in front of the foil will determine the overall image magnification.

Table 1.

Particle	**Energy (MeV)**	**Rate (Ions/sec.)**	**dE/dx (ref) (keV/cm^2)**	**No of (ref) electrons**	**Measured Efficiency(%)**
^{4}He	6.0	~2000	0.75	6	64
^{17}F	180.0	(2-4)*10^6	3.023	20	40 (?)
^{11}Be	880.0	~10000	0.351	2	25
^{18}O	1800.0	~1*10^6	0.39	4	40
^{36}Ar	5400.0	< 1*10^6	1.40	10	100
^{28}Si	120.0	(1-2)*10^6	10.0	~100	100

References:

1) D. Shapira, Nucl. Instrum. Meas. **B204**, 544 (2003).
2) A. N. Stillman et. al, Rev. of Sci. Instrum. **63 (6)**, 3412 (1992).
3) D. Shapira et. al., Nucl. Instrum. Meas. **A400**, 185 (1977).
4) A. N. James et. al., Nucl. Instrum. Meas. **A267**, 144 (1988); O.H. Odland et. al., Nucl. Instrum. Meas. **A378**, 149 (1996).
5) D. Shapira et. al., Nucl. Instrum. Meas. **A449**, 396 (2000).
6) D. Shapira et. al., Nucl. Instrum. Meas. **A454**, 409 (2000).

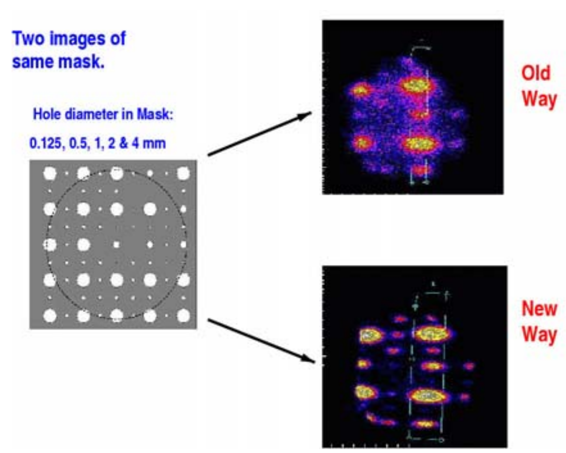

Fig. 8. Two images of the same slit pattern acquired with the detectors shown in Fig. 5 and Fig. 7.